



Research Article

## Impact of air flow, temperature distribution, and heat transmission in a refrigerator compartment with and without shelves: A numerical approach

Md. Ahsanul BARI<sup>1</sup> , Dipayan MONDAL<sup>1,\*</sup> , Md. Abdul HASIB<sup>1</sup>

<sup>1</sup>Department of Mechanical Engineering, Khulna University of Engineering & Technology, Khulna, 9203, Bangladesh

### ARTICLE INFO

#### Article history

Received: 06 April 2024

Revised: 10 September 2024

Accepted: 18 September 2024

#### Keywords:

Air Flow; ANSYS Workbench 2020 R1; Heat Transmission; Refrigerator Compartment (with and without shelves); Temperature Distribution

### ABSTRACT

This study explores the impact of shelf configurations on airflow, temperature distribution, and heat transfer within a refrigerator's compartment, aiming to optimize natural convection for enhanced energy efficiency and preservation. This analysis assumes a steady-state and laminar air flow to maintain a constant heat transfer rate, where the flow is to be stable with a consistent two-dimensional pattern. Computational fluid dynamics simulations are conducted with ANSYS Workbench 2020 R1 to model airflow patterns, temperature gradients, and heat transfer mechanisms under various shelf configurations. The effect of shelves on airflow and temperature distribution inside the refrigerant compartment are investigated and compared the results of temperature and air-flow distribution by altering the number of glass plates. The analysis reveals significant temperature stratification: colder air tends to settle at the bottom, while warmer air accumulates at the top. Glass shelves are found to disrupt the primary airflow along the walls, but they also enhance heat transfer by improving airflow near the walls. This results in higher temperatures in the upper sections of the refrigerator compared to the average, which presents challenges for storing temperature-sensitive items regardless of the shelf configuration. The lowest temperature in the compartment is 272.55 K at 0~10 cm from the bottom wall, and the highest is 279.75 K at 95~100 cm, due to the upward rise of hot air and downward sink of cold air. The pressure ranges are from  $-7.11 \times 10^{-3}$  to  $2.88 \times 10^{-1}$  Pa for without shelves and  $-7.95 \times 10^{-3}$  to  $3.07 \times 10^{-1}$  Pa with four shelves, respectively. Maximum air velocities are  $1.87 \times 10^{-2}$  m/s for without shelves and  $1.61 \times 10^{-2}$  m/s for with shelves. By measuring temperatures, pressure, and air velocities at various points within the compartment maintained at the optimal temperature, the study highlights the impact of air density changes on airflow and temperature distribution. The findings underscore the importance scope of shelf design and placement in minimizing temperature differentials and improving cooling efficiency. The originality of this work lies in advancing beyond conventional forced convection models by exploring temperature stratification and natural convection effects to optimize shelf layout and improve energy efficiency. This study integrates detailed air flow analysis with practical implications for refrigerator design, advancing beyond conventional forced convection systems. Future research could explore alternative shelf materials, optimal configurations, and consumer behavior to further refine refrigeration technologies for sustainable household use.

**Cite this article as:** Bari A, Mondal D, Hasib MA. Impact of air flow, temperature distribution, and heat transmission in a refrigerator compartment with and without shelves: A numerical approach. J Ther Eng 2024;10(6):1590–1606.

#### \*Corresponding author.

\*E-mail address: [dipkuet@me.kuet.ac.bd](mailto:dipkuet@me.kuet.ac.bd)

This paper was recommended for publication in revised form by Editor-in-Chief Ahmet Selim Dalkılıç



## INTRODUCTION

In today's world, the refrigerator is essential to every household daily for keeping food and other perishable goods at a low temperature to prevent the growth of injurious bacteria and other microbes. The working mechanism of the refrigerator is to transfer heat from the interior to the exterior using a refrigeration cycle by circulating a working fluid, either gas or liquid, through a series of coils and compressors. Usually, the refrigerated interior is kept at a temperature between 1–5°C (33–41°F) by adjusting it to the desired temperature to maintain the quality and safety of food for a longer period. One of the refrigerators currently in high demand is the frost-free refrigerator with its large storage capacity, quick chilling, and automatic defrosting [1]. Although the average household's standard temperature is 4°C, a survey found that 26% of refrigerators run at an average temperature higher than 8°C [2–4]. One predominant mode of heat transfer within refrigerators is natural convection, which plays a critical role in the storage and transport of food products. This is especially true for domestic refrigerators, unventilated cold rooms, and during the handling of food pallets, where heat exchange with the ambient air is prevalent. However, domestic refrigerators often suffer from elevated temperatures due to inadequate heat dissipation. The market offers two main types of refrigerators: static and ventilated. In static refrigerators, heat transfer predominantly occurs through natural convection due to the absence of ventilation systems [5].

Numerous studies have been conducted to determine how to enhance the thermal homogeneity within a refrigerator compartment. Karayiannis et al. [6] provided a comprehensive analysis of natural convection in single and two-zone rectangular enclosures, while Betts and Bokhari [7] reported an experimental investigation of turbulent natural convection in a confined, tall chamber to provide information for the validation of computational models consisting of a rectangular cavity with a height-to-width aspect ratio of 6:1. Bansal et al. [8] presented a detailed analysis of the design and performance of egg-crate-type evaporators that can achieve up to 20% improvement in cooling capacity and energy efficiency compared to a standard design. Additionally, they provided a numerical analysis of the refrigeration systems' mass and heat transport. Masjuki et al. [9] provided an overview of ISO energy test specifications for refrigerators and also freezers, which involve measuring energy consumption, cooling capacity, and other performance characteristics. Laguerre and Flick [3] described the numerical model used to simulate the airflow and heat transfer within the refrigerator, including velocity and temperature distributions, pressure drops, and the heat transfer coefficients of the various components. Ding et al. [10] sought to enhance the refrigerator's internal temperature homogeneity, which is essential for preserving the food's freshness and quality. Hermes et al. [11] developed a useful tool for assessing the energy efficiency of household freezers and refrigerators that affect the different design factors on the energy usage of refrigeration appliances.

Yang et al. [12] investigated a frequently used top-mounted type of household refrigerator to optimize the design of the refrigerator and assess its energy efficiency through conducting experimental tests. Bayer et al. [13] focused on analyzing the thermal performance of a refrigerator compartment while taking radiation effects into account utilizing reduced order models and computational fluid dynamics (CFD) simulations. Yan et al. [14] investigated the freezer gasket's thermal load and heat transmission characteristics in refrigerators showing the temperature distribution and heat flux in the gasket by designing a test rig and creating a numerical model using the finite element method. Avci et al. [15] conducted a comprehensive study on the optimization of household refrigerator design parameters using artificial neural networks (ANNs) and CFD simulations, while Gao et al. [16] conducted a comprehensive investigation on heat leakage at the gasket region of a refrigerator using both experimental and numerical methods. The experimental and modeling investigation of a small-capacity dynamic diffusion-absorption refrigerator was detailed by Mansouri et al. [17], whereas Ledesma and Belman-Flores [18] employed a model to study about thermal performance of the household refrigerator and explore the impact of shelf placement on its behavior. Moreover, Söylemez et al. [19] conducted a comprehensive study on a refrigerator system that integrates vapor compression cooling with thermoelectric systems. Gulmez and Yilmaz [20] conducted a comprehensive investigation into developing and designing a condensation-preventing door gasket for refrigerators. Li et al. [21] aimed to develop a novel air distributor for multi-compartment indirect cooling household refrigerators, providing more precise control of cooling capacity delivery. The research by Wie et al. [22] utilized CFD simulations to evaluate the temperature homogeneity of a household refrigerator for various duct configurations. Logeshwaran and Chandrasekaran [23] also conducted CFD simulations to analyze the heat transfer that occurs via natural convection and to identify the impact of different factors, including the position of the evaporator and the compartments' shape. Cui et al. [24] conducted a numerical investigation of the flow and heat transfer in a domestic refrigerator with complex wall conditions. They aimed to analyze the effect of wall geometry on the cooling performance of the refrigerator to enhance the design of more efficient refrigeration systems.

Furthermore, Jalili and Jalili [25] examined how the severity of airflow turbulence affected the penetration and breakup of liquid jets in two-phase cross-flows when numerical solutions were obtained using the large-eddy simulation approach. The level set model and volume of fluid (VOF) model are combined for two-phase crossflow modeling. A study by Jalili et al. [26] discussed the analysis of a geothermal system's convective-conductive heat transfer phenomena, while Jalili et al. [27, 28] reported using nano-fluid for the examination of the pressure drop and thermal analysis in the curved rectangular fin on the heat transfer of a double-pipe heat exchanger and the non-continuous helical baffle with varying helix angles, respectively. Moreover, Salehipour et al. [29] explored the

impact of combustion product humidification on the spiral geometry boiler economizer and Sun et al. [30] reported the heat transfer performance prediction of Taylor–Couette flow with longitudinal slits using artificial neural networks. Mondal et al. [31, 32] reported the experimental observation of a small capacity vapor absorption cooling system and bend tube water to the air heat exchanger, while Mondal and Islam [33] investigated the intermittent ammonia absorption refrigeration system. To suit the low GWP refrigerant in air conditioning and refrigeration systems, the transport properties of low GWP refrigerants are measured by Mondal et al. [34–38] which will assist in choosing the refrigerant for the useful appliance. Yilmaz et al. [39] investigated the bottom cabinet-type household refrigerator which formed in two stages including the fan motion and the heat rejection process at the condenser, respectively. Roy and Kundu [40] proposed a thermodynamics model of a pulse tube-type refrigeration system utilizing the optimum gas behavior to calculate the refrigerator's cooling effect, while Choudhari et al. [41] offered an approach to second-order cyclic analysis which developed a model to evaluate the performance (refrigerating effect, power input, and losses individually of each component) of the counter-flow pulse tube refrigerator. Ozkan and Unal [42] proposed to reduce energy usage and boost the defrosting process' effectiveness in refrigerators without a frost, while Shikalgar and Sapali [43] described a home refrigerator using a box-style shell and tube water-cooled condenser and a hot-wall air-cooled condenser. Exergy losses in the refrigerator can be localized with the aid of energy and exergy analysis techniques. The purpose of this study was to calculate the coefficient of performance, energy efficiency, and energy loss in each component of the household refrigerator using the same refrigerator unit but a different condenser. Meanwhile, Kumar et al. [44] conducted a comparison of cascade refrigeration systems employing various refrigerant combinations based on energy and exergy using the mathematical simulation using Engineering Equation Solver. Another study by Arslan et al. [45] proposed an experimental study for thermodynamic analyses of energy, exergy, and environment using several refrigerants for a supermarket application to use in the microchannel in order to increase the cooling efficiency of the system. Gugulothu [46] proposed a household refrigeration system to enhance energy efficiency by adjusting the length of the capillary tube and the refrigerant charging effect. Illyas et al. [47] conducted a CFD analysis that showed peak heat transfer at 30° and 45° rib angles and the highest exergy loss at a 60° rib angle in a square duct with six truncated and circular ribs. A study was conducted by Shariar et al. [48] where three different dehumidifier plate configurations were used to show the impact of gas-liquid flow on liquid LiCl desiccant dehumidifier performance. In the test section, the desiccant flows downwards for gravitational force, and airflow is to be set opposite to the desiccant flow from vertically downward to upward. Then, the amount of moisture collected from the air was investigated by the simulation using ANSYS workbench 2020 R1. Meanwhile, Hmood et al. [49] dropped in and retrofitted the refrigerants

as a replacement for R134a in refrigerator and automobile air conditioner applications to assess the effectiveness of a range of environmentally friendly substitutes. Gambhir et al. [50] used response surface methodology to study the thermodynamic optimality of a double-effect vapor absorption refrigeration system powered by blowdown heat from a 210 MW thermal station at Badarpur. Deshmukh et al. [51] implemented a critical evaluation of phase change materials (PCM) in a refrigerator's volumetric cooling capacity (VCC) where integrating PCM with the conventional setup enhances the capacity for heat exchange. Hasheer SK et al. [52] reported a theoretical examination of low GWP refrigerants of pure and mixture as the replacement of R134a in the VCR system. The performance of a home refrigerator was measured using the compressor discharge temperature, COP, VCC, refrigerant mass flow rate, compressor power consumption, and pressure ratio. Ugudur and Direk [53] carried out an experimental ejector refrigeration system for various operating modes in order to gauge the system's effectiveness. The findings demonstrated that the dual-evaporator ejector system mode produced the highest total cooling capacity and COP, whereas the conventional dual-evaporator system mode produced the lowest total cooling capacity. Moreover, Shahini et al. [54] assessed the evacuated tube solar collectors' direct absorption energy study employing  $\text{Al}_2\text{O}_3$  nanoparticles is investigated numerically. Another study by Islam et al. [55] presented a numerical study of the properties of heat transfer for R32 and R1234yf using  $\text{Al}_2\text{O}_3$  nanoparticles via a U-bend evaporator for refrigerator where mapping the flow pattern and estimating the pressure drop are also performed. Srivastava and Maheshwari [56, 57] performed the thermodynamic analysis of solar assisted binary vapour cycle using ammonia-water mixture and transcritical  $\text{CO}_2$ . Meanwhile, Amin [58] developed a new combined cascade absorption-adsorption refrigeration system (ABS-ADS). Compared to other earlier studies, the cascade ABS-ADS cycle that has been proposed can function well at low-grade heat sources and generate good thermal performance.

From the aforementioned debate, several research studies were performed to explore the efficiency of a refrigerator which is influenced by various factors, including design, insulation materials, and the cooling system. A critical aspect of refrigerator design is the analysis of airflow and heat transfer. To date, little to no research has been done taking the research on airflow distribution, temperature distribution, and heat transfer rates inside the compartments of domestic refrigerators. By analyzing the effect of door openings on airflow patterns and temperature distribution internal compartment of a refrigerator, it is understood how frequent access impacts thermal stratification and energy consumption could lead to practical recommendations for users to maintain optimal storage conditions. To explore optimal shelf configurations and placements within the refrigerator, it needs to minimize temperature differentials and enhance overall cooling efficiency. Therefore, the targets of this are to analyze the distribution of temperature and air flow in a model refrigerator, focusing on natural convection systems

rather than forced convection systems. The originality of this work lies in its detailed CFD analysis of how different shelf configurations affect airflow and temperature distribution in a refrigerator’s compartment. It advances beyond traditional forced convection models by exploring natural convection effects and temperature stratification, providing new insights for optimizing shelf design and improving energy efficiency. The study also seeks to determine the optimal temperature at various points within the compartment to maintain quality while minimizing electricity usage. In static refrigerators, variations in air density affect the distribution of temperature and airflow, and external conditions can affect the transfer of heat during natural convection in the refrigerating compartment. The simulation will examine precise airflow and temperature distribution to enhance system efficiency.

**METHODOLOGY**

A static refrigerator with and without glass shelves was used in this study. The model refrigerator that was used for the study only had a refrigerating chamber and one door. It

did not have a freezer. Here, two cases were studied. Figure 1 depicts two different empty refrigerators: one without glass shelves, and another with glass shelves. The refrigerating compartment is treated as a 2D object to avoid the complicity of the geometry. The temperature distribution inside a refrigerating compartment with no freezer was assumed to be a rectangular enclosure with an evaporator wall and a door. The right-side wall is supposed to be a warm wall (door), while the left side is assumed to be a cold wall (evaporator). The dimensions of the refrigerant compartment are given in Table 1.

**Table 1.** Dimensions of the refrigerator model

SL	Content	Value
1	External dimensions	110 × 60 × 60 (cm <sup>3</sup> )
2	Internal dimensions	100 × 50 × 50 (cm <sup>3</sup> )
3	Number of shelves	4
4	The thickness of glass shelves	5 (mm)

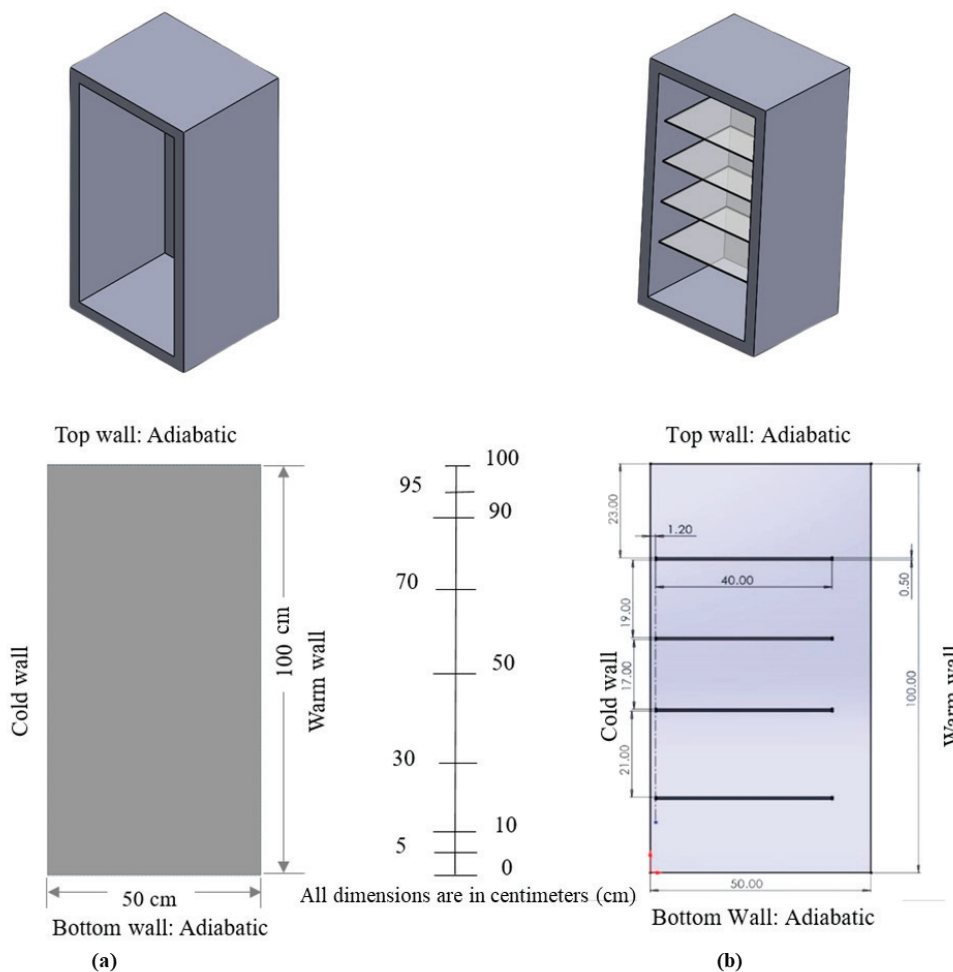


**Figure 1.** Sketch for the refrigerating compartment; (a) without shelves, and (b) with shelves.

**Table 2.** Numerical setup and solver setting

Parameter	Setup	Parameter	Value
Solver Type	Pressure-based	Specific heat ( $J kg^{-1} K^{-1}$ )	1006.43
Time	Steady	Thermal conductivity ( $w m^{-1} K^{-1}$ )	0.0242
Viscous Model	Laminar	Viscosity ( $kg m^{-1} s^{-1}$ )	$1.7894 \times 10^{-5}$
Fluid	Air	Thermal expansion	$3.66 \times 10^{-3}$
Density	Boussinesq approx.	Molecular weight ( $kg K^{-1} mol^{-1}$ )	28.966

### Formation of the Problem

In the current study, simulations were performed using ANSYS Additive 2020 R1. As the flow is steady and laminar, a pressure-based solver was chosen. The energy equation was also enabled. The flow was assumed to be stable in the simulation process, with a consistent direction and two-dimensional. For the numerical simulations, a simple scheme is employed for pressure and velocity coupling, ensuring robust and stable calculations. The Green-Gauss cell-based method is used for gradient calculations, while the PRESTO scheme is applied for pressure interpolation. To enhance the accuracy of the results, the second-order upwind scheme is utilized for both momentum and energy equations, effectively minimizing numerical diffusion. The Boussinesq approximation was also taken into account during the simulation. The governing equations [59] used to represent fluid flow in Cartesian coordinates were the two-dimensional Continuity, Navier-Stokes, and Energy:

$$\frac{\partial u}{\partial x} + \frac{\partial v}{\partial y} = 0 \quad (1)$$

$$u \frac{\partial u}{\partial x} + \frac{\partial u}{\partial y} = \frac{\partial p}{\partial x} + \vartheta \left( \frac{\partial^2 u}{\partial x^2} + \frac{\partial^2 v}{\partial y^2} \right) \quad (2)$$

$$u \frac{\partial v}{\partial x} + \frac{\partial v}{\partial y} = \frac{\partial p}{\partial y} + \vartheta \left( \frac{\partial^2 u}{\partial x^2} + \frac{\partial^2 v}{\partial y^2} \right) \quad (3)$$

$$u \frac{\partial T}{\partial x} + \frac{\partial T}{\partial y} = \alpha \left( \frac{\partial^2 u}{\partial x^2} + \frac{\partial^2 v}{\partial y^2} \right) \quad (4)$$

where  $u$  and  $v$  are the velocity components, and  $\vartheta$  and  $\alpha$  are the kinematic viscosity and thermal diffusivity. Several Rayleigh numbers ( $R_a = 10^4 \sim 10^6$ ) are simulated for the study; this Rayleigh number is distinct by the equation:

$$R_a = \frac{g\beta(T_H - T_C)L^3}{\vartheta\alpha} \quad (5)$$

where  $\beta$  and  $L$  are the thermal expansion coefficient and distance from the hot to cold wall. The diverse value of  $R_a$  was achieved by changing the gravitational acceleration ( $g$ ). Also, the local Nusselt number ( $Nu$ ) and average Nusselt number ( $Nu_{av}$ ) were estimated with the equations:

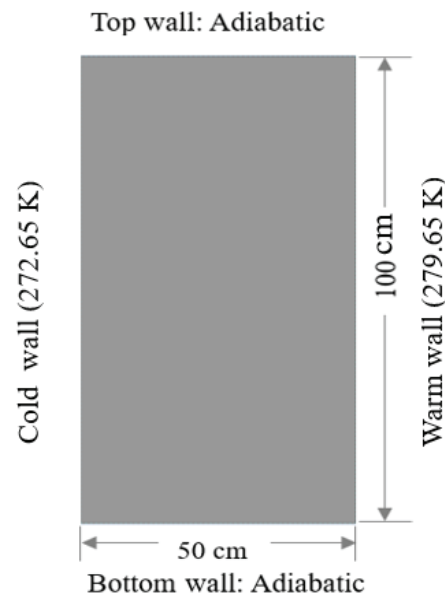
$$Nu = \frac{hL}{k} \quad (6)$$

$$Nu_{av} = \frac{1}{L} \int_0^L Nu dy \quad (7)$$

where  $h$  is the convection heat transfer coefficient and  $k$  is the thermal conductivity. Previously informed that this numerical problem is solved with a density-based solver by ANSYS Additive 2020 R1 and hence, the numerical setup is listed in the following Table 2.

### Boundary Conditions

To make the study easier to understand, a few assumptions have been made. First, a well-sealed compartment is implied by the assumption that there is no mass flow rate through the boundaries. The air velocity at the walls is set to zero, in accordance with the no-slip requirement, which accurately reflects the physical behavior of air in contact with solid surfaces. The analysis assumes a steady-state and laminar air flow to maintain a constant heat transfer rate, with the Rayleigh number kept below  $10^9$ , ensuring the

**Figure 2.** Boundary conditions for this study.

flow regime remains laminar. Additionally, the effects of radiation are neglected, focusing the study on conduction and convection as the primary modes of heat transfer. The temperature boundary conditions are set with the cold wall (evaporator) maintained at 272.65 K and the warm wall at 279.65 K, respectively, representing typical operating conditions within a refrigerator. Both the upper and bottom walls are considered adiabatic shown in Figure 2, implying no heat transfer occurs through these surfaces, thereby simplifying the thermal analysis.

### Grids Independence Test and Validation

In order to enhance wall function and better convergence for the empty refrigerating compartment, the non-uniform structural mesh was generated for this study by ANSYS mesh with a maximum resolution close to the wall. Figure 3 shows the meshed refrigerating compartment for one without glass shelves and another with glass shelves. It is considered for selecting the element types, a region with complex geometries, such as around the shelves and intricate internal structures, tetrahedral elements are used that offer flexibility in fitting irregular shapes and provide a good balance between accuracy and computational efficiency. For more regular and less complex regions, hexahedral elements are utilized and for the near-wall regions, especially adjacent to the evaporator and other heat-exchanging surfaces, prismatic (wedge) elements are meshed that help in accurately resolving the boundary layers and crucial for capturing heat transfer and fluid flow dynamics

near walls. While selecting the element sizes, a finer mesh is employed near the walls, shelves, and critical heat exchange areas. The near-wall mesh is refined to ensure that the boundary layer is adequately resolved, typically with a first cell height small enough to capture the temperature and velocity gradients accurately. In the central regions of the compartment, where the gradients are less steep, a coarser mesh is used for reducing the overall computational load without significantly compromising the accuracy of the simulation. Again, smooth transition zones are established between fine and coarse mesh regions to prevent numerical instabilities and ensure a seamless flow of information across different mesh densities. But face meshing and edge sizing were done to improve mesh quality for the refrigerating compartment with shelves. The mesh independence test was carried out using a series of simulations for refrigerating compartments without and with shelves. By dividing rectangular sections of the compartment with different edge sizing, a different number of meshes were developed. These simulations were carried out for compartments with and without shelves.

The simulation was conducted until the average Nusselt number ( $Nu_{av}$ ) reached a constant value, as indicated by Table 3, which also displays the convergence conditions that were set for this study. Meanwhile, Figure 4 shows that the Nusselt number varies with the number of mesh elements for  $Ra = 10^5$  for the zero-degree angle of rotation. The meshes of more than 10000 elements can produce accurate results with minimal deviation for without selves,

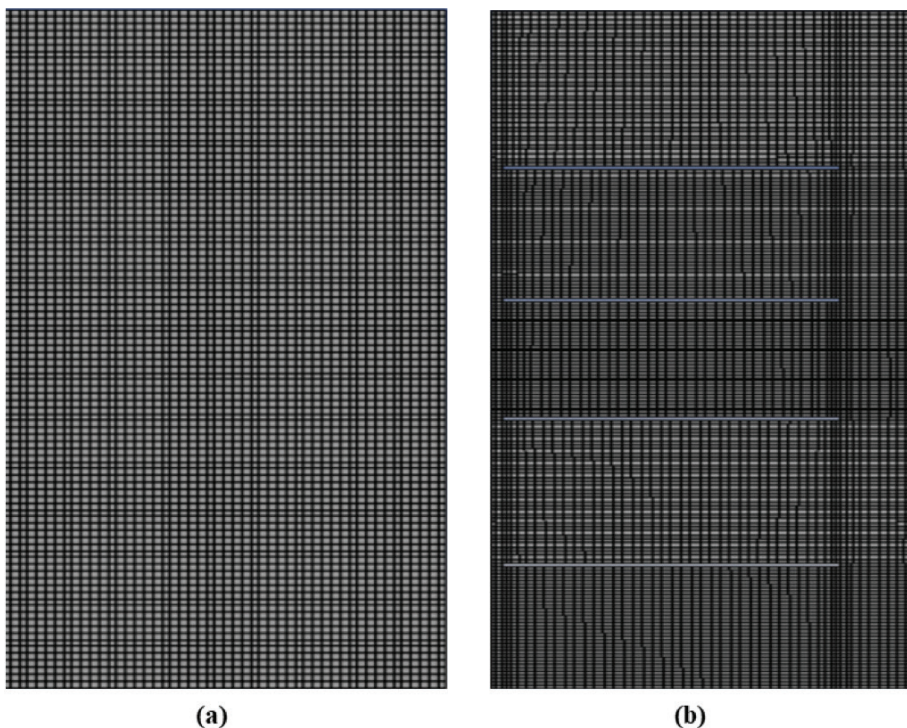


**Figure 3.** Meshed refrigerating compartment (a) without shelves, and (b) with shelves.

**Table 3.** Comparing current and earlier studies on square cavities as refrigerating compartments (Nusselt number based on Rayleigh number)

Research	Ra = $10^4$	Ra = $10^5$	Ra = $10^6$
This work	2.275	4.651	8.893
Inam [59]	2.247	4.535	8.855
Davis [60]	2.243	4.519	8.799
Rincon- Casado et al. [61]	2.241	4.522	8.819

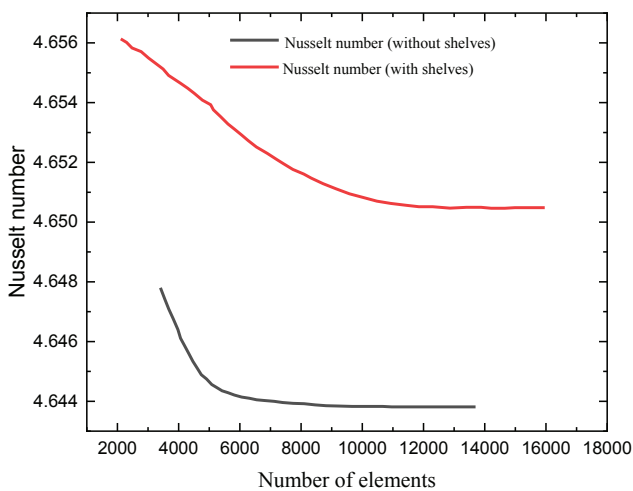


**Figure 4.** Mesh independence test.

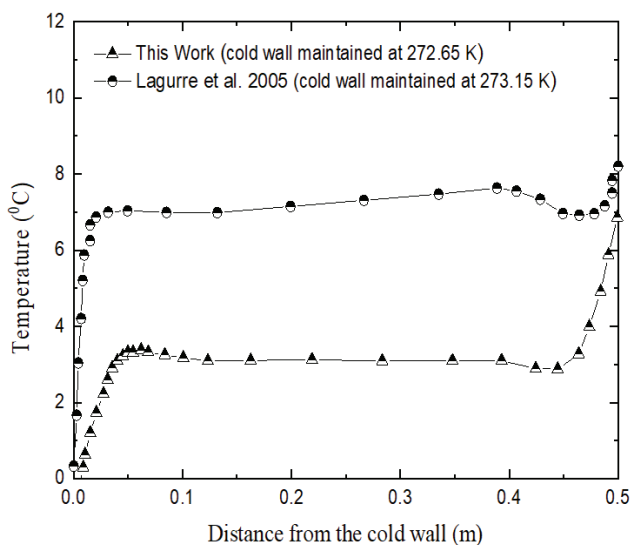


**Figure 5.** Comparison of horizontal temperature profiles at mid-height (50 cm) of refrigerator model of this work maintained at cold work at 272.65 K and Laguerre et al. [5] at cold wall maintained at 273.15 K, respectively.

and more than 13000 elements can produce accurate results with minimal deviation for with shelves. As a result, for further simulation, the mesh with element number 10450 was chosen for the compartment without shelves, and 13020 was chosen for with shelves to obtain the good outcomes of this work. Moreover, Figure 5 displays the fluctuation of a refrigerator model's horizontal temperature profiles at mid-height (50 cm). In this work, the cold wall is maintained at 272.65 K, whereas in Laguerre et al. is maintained at 273.15 K for the cold wall temperature, respectively. Despite different boundary conditions, this work and Laguerre et al. [5] have noticed almost similar trend findings which indicate justification of the suitable model.

## RESULTS AND DISCUSSION

### Effect of Temperature Distributions

The simulation considered the heat transfer that occurs through natural convection between the different sides of the compartment and the airflow within the refrigerating compartment. Figure 6 represents the temperature distributions at different points of the refrigerating compartment without and with shelves. The simulation results showed that in an empty refrigerating compartment without a freezer, there was a difference in temperature between the top and bottom regions, indicating thermal stratification. With the presence of shelves, the temperature at the bottom was lower, while at the top, it was slightly higher compared to the compartment without shelves. Additionally, the shelves reduced airflow in the middle of the compartment, which affected air circulation on the evaporator and isothermal walls. The simulation also revealed thermal stratification in each gap between the shelves with increasing air temperatures as the number of shelves increased. By measuring temperatures at various points within the compartment maintained at the optimal temperature, the study highlights the impact of air density changes on airflow and temperature distribution. The obtained temperatures of this study are noticed at 279.75 K for the warm wall, and 272.55 K for the cold wall, respectively. These findings emphasize the significance of considering the design of the refrigerating compartment and its components to improve the efficiency of refrigeration systems. While the separate study by Laguerre et al. [2] and Logeshwaran and Chandrasekaran [23] reported the simulation for heat transfer in refrigerators without shelves, two and four shelves got almost similar trends of results.

Figure 7 illustrates the horizontal temperature profile over the heights from the bottom to the top wall of the refrigerating compartment without and with shelves, respectively. The temperature closest to the cold wall is likely the lowest, as heat is transferred from the warmer air to the colder wall. As the air travels upward, heat is transferred back into the air, causing the temperature to increase away from the cold wall. The temperature profiles were

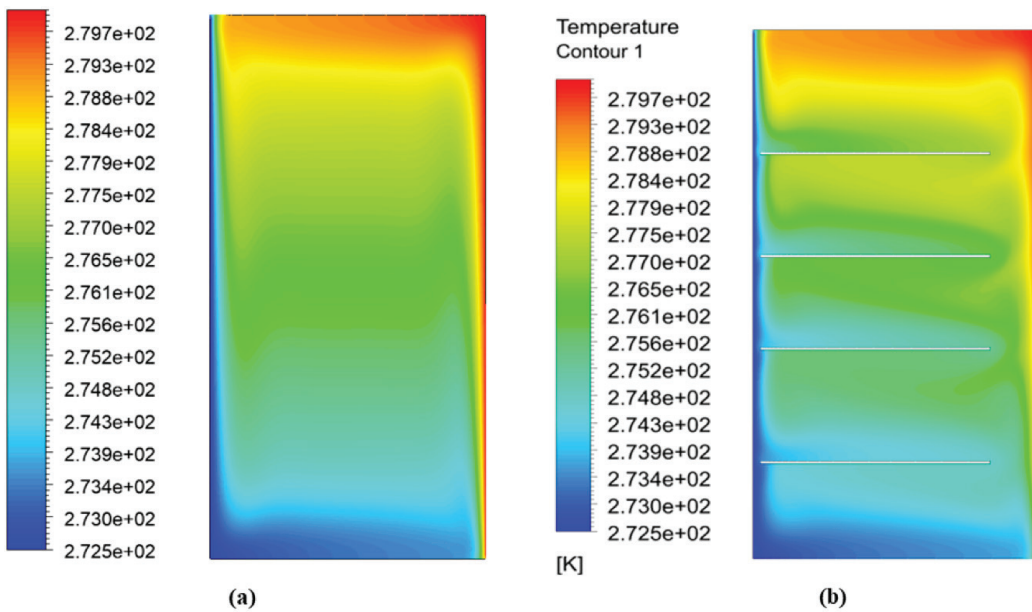


**Figure 6.** Temperature distributions within the refrigerator at several locations; (a) without shelves, and (b) with shelves.

measured at different heights (i.e., 0 cm, 5 cm, 10 cm, 30 cm, 50 cm, 70 cm, 90 cm, 95 cm, 100 cm) from the bottom wall.

Figure 7(a) illustrates the temperature profile over the heights from the bottom wall of the refrigerating compartment without shelves. Heat rises, which can cause differences in temperature at different heights, with the warmer air at the bottom not mixing as readily with the cooler air at the top. Between the distances of 0.03 cm to 0.43 cm from the cold wall to the hot wall, the temperature increases rapidly from the bottom to the top. The temperature is the lowest of 272.55 K at 0 cm height from the bottom wall and highest of 279.75 K at 100 cm height from

the bottom wall because the hot air rises upward and the cold air sinks downward, creating density variations in the compartment. Meanwhile, Figure 7(b) shows that shelves inside the refrigerating compartment alter the natural convection heat transfer and airflow, causing temperature variations. The temperature is the lowest of 272.55 K at 0 to 5 cm from the bottom wall and highest of 279.75 K at 95 to 100 cm from the bottom wall. The presence of shelves lowers the temperature at the bottom of the compartment, where the shelves block the airflow, resulting in less heat transfer from the walls to the air. Conversely, at the top of the compartment, the temperature is slightly higher due to

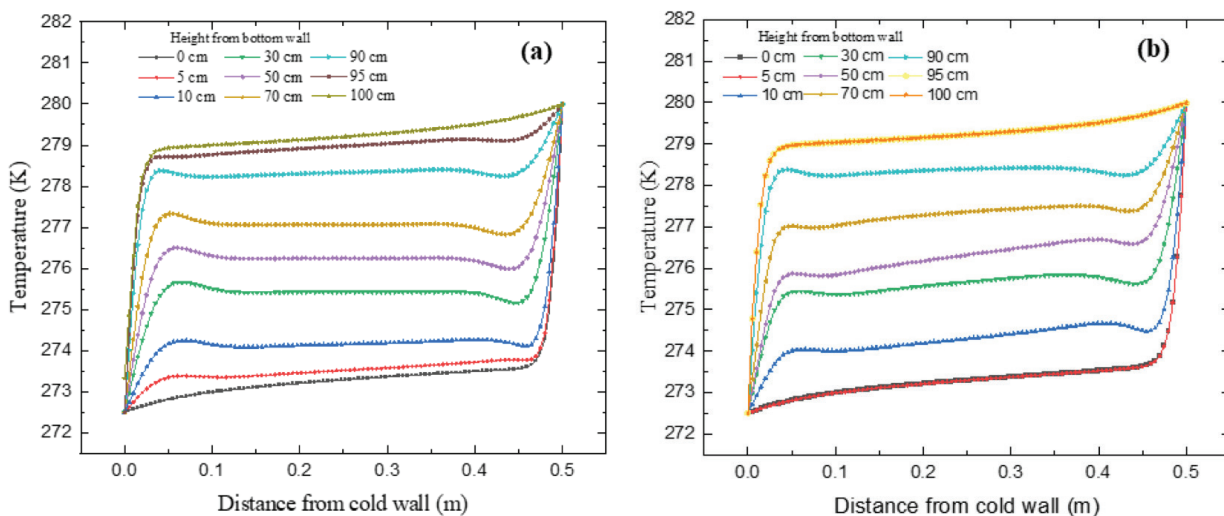


**Figure 7.** Temperature profile over the heights from the bottom wall of the refrigerating compartment; (a) without shelves, and (b) with shelves.



reduced air flow in the middle of the compartment caused by the presence of shelves. This increased airflow at the top improves heat transfer from the walls to the air, resulting in a slightly higher temperature at the top of the compartment compared to the case without shelves.

Moreover, comparing the horizontal temperature profiles of a refrigerator model at 50 cm (mid-height) previously shown in Figure 5, the cold wall is maintained at 272.65 K, and Laguerre et al. [5] is maintained at 273.15 K for the cold wall temperature, respectively. Despite different boundary conditions, this work and Laguerre et al. have noticed almost similar trend findings which indicate justification of the suitable model.

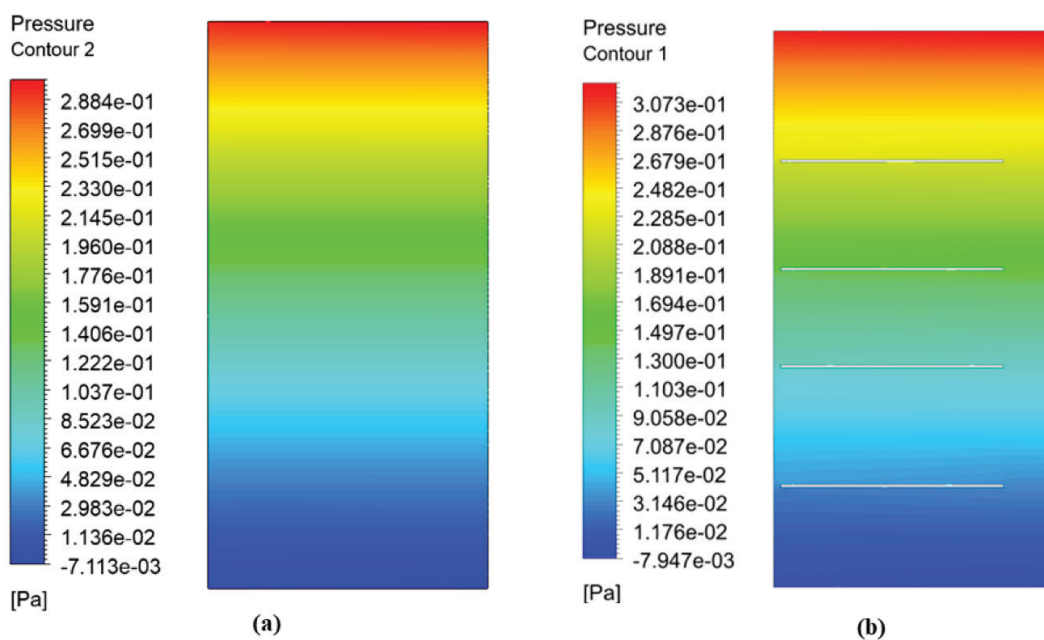
### Effect of Pressure Variations

The pressure and temperature distribution within the compartment of the refrigerator is affected by the airflow, which is influenced by changes in air density. Figure 8 demonstrates the pressure distribution in the refrigerant compartment for an empty compartment without shelves and a compartment with shelves, revealing that the bottom has low pressure while the top has high pressure. These pressure differences result from temperature variations, with colder air being denser than warmer air, thus leading to air circulation. The pressure range that was obtained in the refrigeration compartment without shelves and with four shelves is seen as  $-7.11 \times 10^{-3}$  to  $2.88 \times 10^{-1}$  Pa and  $-7.95 \times 10^{-3}$  to  $3.07 \times 10^{-1}$  Pa, respectively. While Logeshwaran and Chandrasekaran [23] for two shelf compartments are found as  $2.80 \times 10^2$  Pa. The air pressure in the compartment with shelves is higher than in the compartment without shelves because impediments like shelves cause the air pressure to

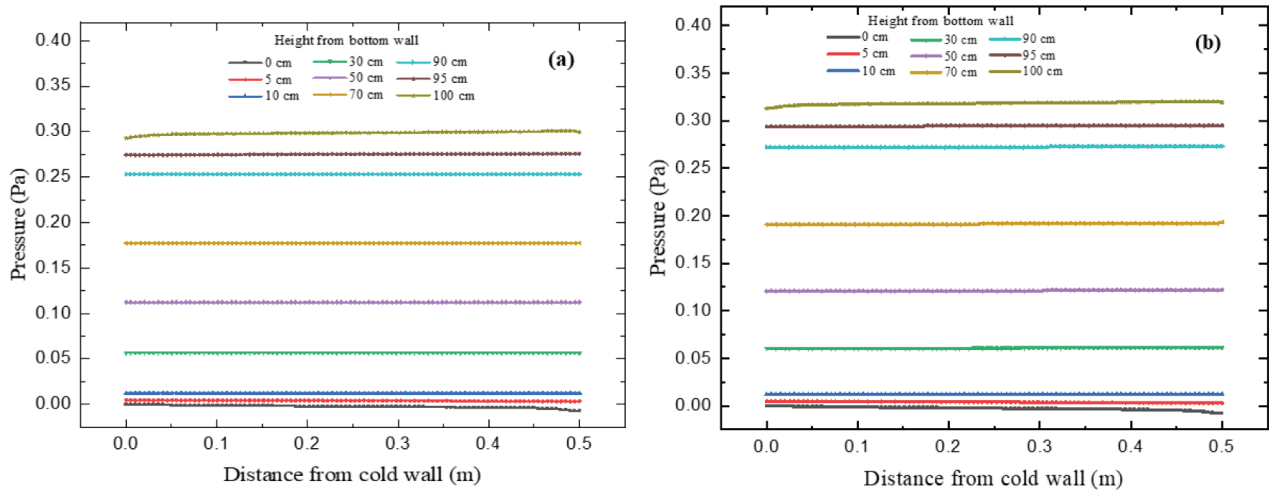
rise. Additionally, the presence of shelves affects the velocity variation within the refrigerating compartment, with air pressure increasing from the bottom of the compartment toward the top.

Figure 9 shows the pressure variations at the different heights (i.e., 0 cm, 5 cm, 10 cm, 30 cm, 50 cm, 70 cm, 90 cm, 95 cm, and 100 cm) from the bottom wall of the compartment without and with shelves, respectively. The pressure at different heights does not vary more along the distance from the cold wall to the warm wall. Here, the pressure increases from the bottom wall to the top. At the bottom, the pressure is very low, and at the top, the pressure is more than the pressure at the bottom. For the refrigerating compartment without shelves, the lowest pressure is  $-7.11 \times 10^{-3}$  Pa at the height of 0 cm from the bottom wall and the highest is  $2.88 \times 10^{-1}$  Pa at the height of 100 cm from the bottom wall.

On the contrary, for the refrigerating compartment with shelves, the lowest pressure is  $-7.95 \times 10^{-3}$  Pa at the height 0 cm from the bottom wall and the highest is  $3.07 \times 10^{-1}$  Pa at the height of 100 cm from the bottom wall. There is a slight increase in pressure in the refrigerating compartment with shelves at the top compared to a refrigerator compartment without shelves. The presence of obstacles (shelves) near the cabin increases the air pressure, leading to greater air pressure at the top of the cabin with shelves compared to the cabin without shelves. However, the pressure is almost the same at the bottom for refrigerating compartments without and with four shelves, while there is a slight difference found in another study by Logeshwaran and Chandrasekaran [23] for two shelves compartments.



**Figure 8.** Pressure variations within the refrigerator at several locations; (a) without shelves (b) with shelves.



**Figure 9.** Pressure variations over the heights from the bottom wall of the refrigerating compartment; (a) without shelves, and (b) with shelves.

**Effect of Air Flow**

The simulation findings show that the air flow is steady and laminar, which leads to relatively low air velocity. Figure 10 illustrates the velocity vector in the refrigerating compartment without and with shelves. The direction of the velocity vector is towards the warm wall (door) from the cold wall, indicating a unidirectional flow and sometimes occurring flow of convection currents from top to bottom. The velocity magnitude is the highest close to the cold wall and decreases gradually as the temperature rises toward the warm wall. The

presence of adiabatic top and bottom walls is relatively minor in the velocity profile. The force driving the air flow is the pressure difference arising from the temperature difference between the cold and warm walls. The obtained maximum air velocity is found as  $1.87 \times 10^{-2} \text{ m/s}$  and  $1.61 \times 10^{-2} \text{ m/s}$  for without shelves and four shelves compartments, respectively. While the separate study by Laguerre et al. [2] and Logeshwaran and Chandrasekaran [23] reported the simulation for air flow in refrigerators without shelves, two and four shelves have almost similar trends of results.

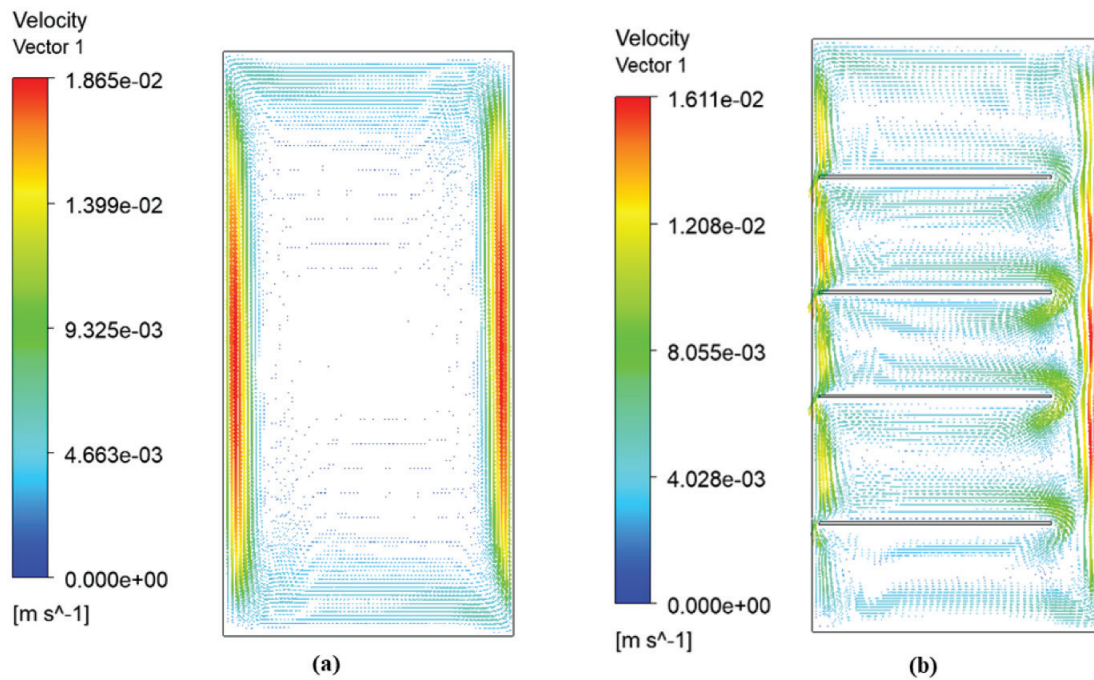


**Figure 10.** Velocity vector in refrigerating compartment; (a) without shelves (b) with shelves.

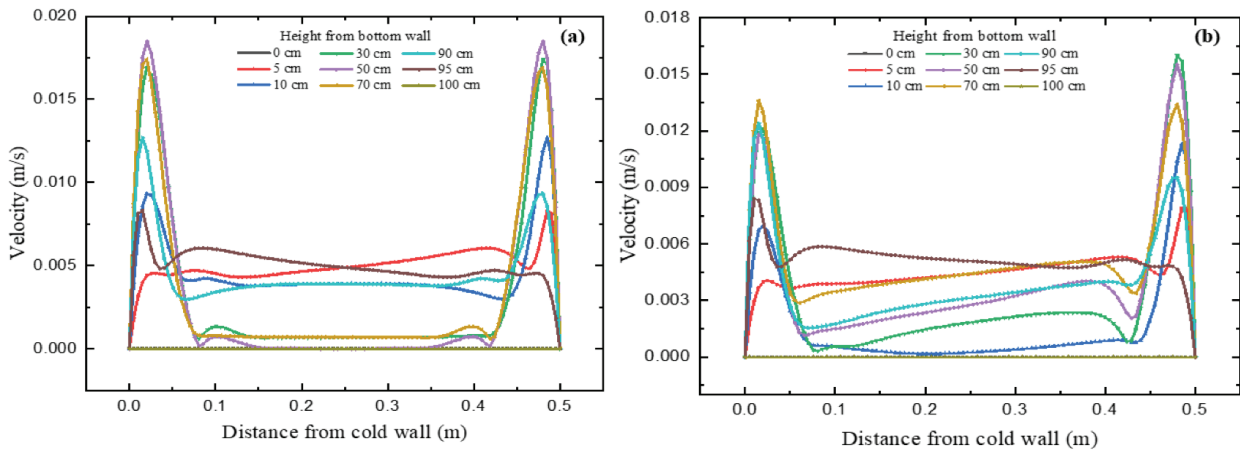


**Figure 11.** Air velocity over the heights from the bottom wall of the refrigerating compartment; (a) without shelves, and (b) with shelves.

Figure 11 represents the air velocity at the different heights (i.e., 0 cm, 5 cm, 10 cm, 30 cm, 50 cm, 70 cm, 90 cm, 95 cm, and 100 cm) from the bottom wall of the refrigerating compartment without and with shelves, respectively. The air velocity near the cold wall and the hot wall are relatively high. A little further away from the cold wall, the air velocity decreases, and then the variation in velocity value is much less. Then the velocity increases as it approaches the hot wall. The air velocity near the hot wall is maximum, and at the bottom wall is almost zero, where also a similar trend is found for the cold wall. In Figure 11(a), the velocity near the cold wall and hot wall at the height of 50 cm from the bottom wall is maximum when there is no shelf in the

refrigerating compartment, and the maximum velocity is obtained as  $1.87 \times 10^{-2} \text{ m/s}$ . In Figure 11(b), the air velocity near the hot wall at the height of 30 cm from the bottom wall is maximum when there are shelves in the refrigerating compartment, and the maximum velocity is  $1.61 \times 10^{-2} \text{ m/s}$ . In comparison, the air velocity near the cold and hot walls is slightly higher in the middle (i.e., 50 cm from the bottom wall) of the refrigerating compartment without shelves compared to the compartment with four shelves. The air-flow in the boundary layers is impacted by the existence of impediments like shelves, which results in more gaps that encourage air circulation and raise air velocity in the middle of the compartment.

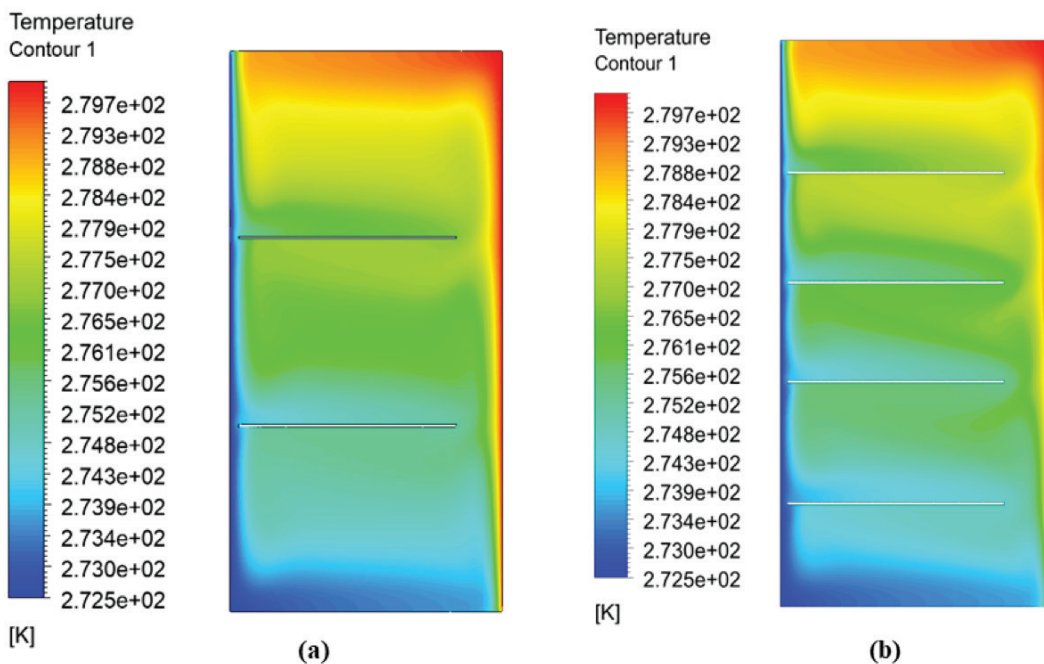
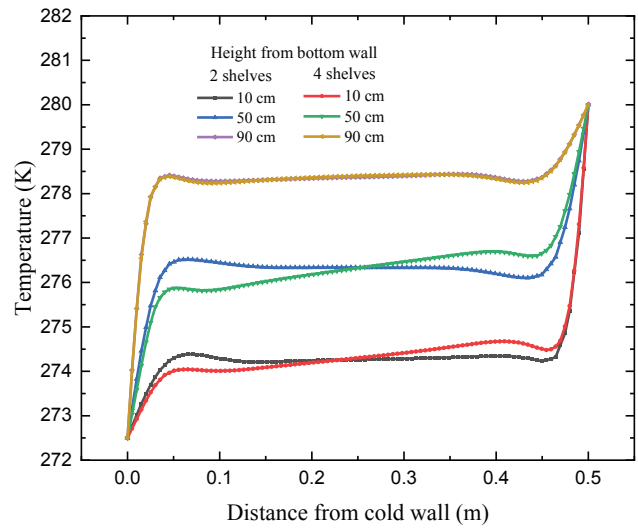


**Figure 12.** Temperature distributions within the refrigerator at several locations; (a) two shelves, and (b) four shelves.

### Comparison Between Refrigerating Compartment with 2 and 4 Shelves

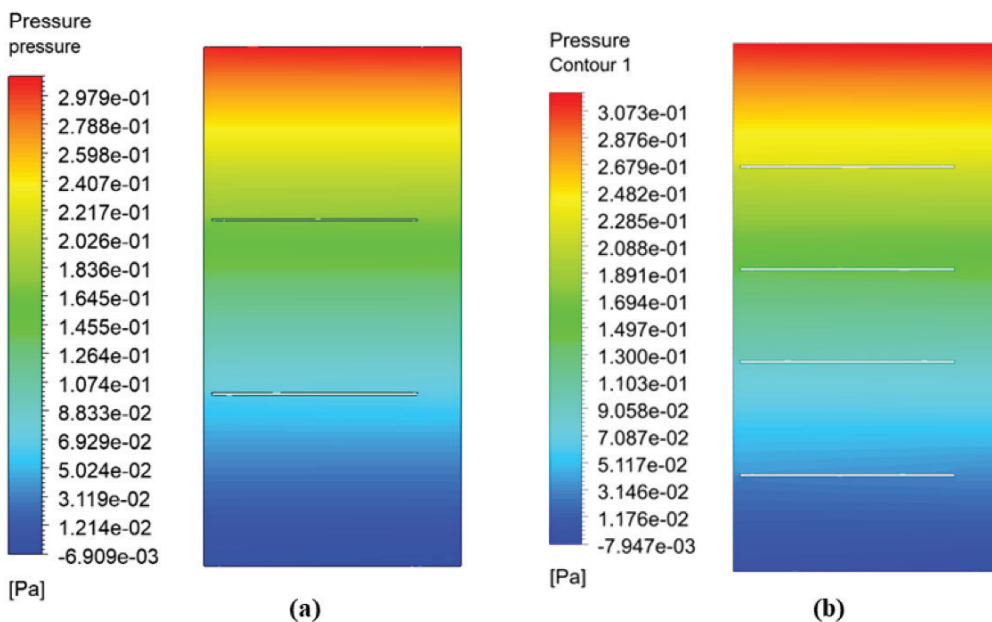
To compare the findings, the temperature distributions, pressure variations, and air flow variations at different points of two shelves and four shelves compartments are investigated in this work, while the separate study by Laguerre et al. [2], and Logeshwaran and Chandrasekaran [23] conducted both for the temperature distribution, pressure variations, and air flow variations for the two and four shelves compartment. The effect of shelves on airflow and temperature distribution inside the refrigerant compartment are investigated and compared the results of temperature and air-flow distribution by altering the number of glass plates. However, Figure 12 shows the temperature distribution for both 2 and 4 shelves from the simulation results that are performed here to compare this work. The upper temperature of the refrigerating compartment is higher and the bottom temperature is lower. However, increasing the number of plates increased the average temperature of the refrigerating compartment.

Figure 13 shows the temperature profile at different heights for the compartment of the refrigerator with 2 and 4 shelves, where the presence of shelves lowers the temperature at the bottom of the compartment, and at the top of the compartment, the temperature is slightly higher due to reduced airflow in the middle of the compartment caused by the presence of shelves. Hence the number of obstacles rises, and there is a corresponding increase in air temperatures. The temperature is the lowest of 272.55 K at 10 cm from the bottom wall and the highest of 279.75 K at 90 cm from the bottom wall for the compartments of 2 and 4 shelves, respectively, because the hot air rises upward and the cold air sinks downward, creating density variations in the compartment.



**Figure 13.** Temperature profile at different heights from the bottom wall in the refrigerating compartment with 2 and 4 shelves.

Figure 14 shows the pressure contours of the refrigerating compartment with 2 and 4 shelves. The maximum pressure of the refrigerating compartment with 2 plates is less than that of the refrigerating compartment with 4 plates. However, the minimum pressure of the refrigerating compartment with 2 plates is more than that of the refrigerating compartment with 4 plates. The obtained pressure range in the refrigerating compartment two shelves and four shelves are noticed as  $-6.91 \times 10^{-3}$  to  $2.98 \times 10^{-1}$  Pa and  $-7.94 \times 10^{-3}$  to  $3.07 \times 10^{-1}$  Pa, respectively.



**Figure 14.** Pressure variations in the refrigerating compartments; (a) 2 shelves, and (b) 4 shelves.

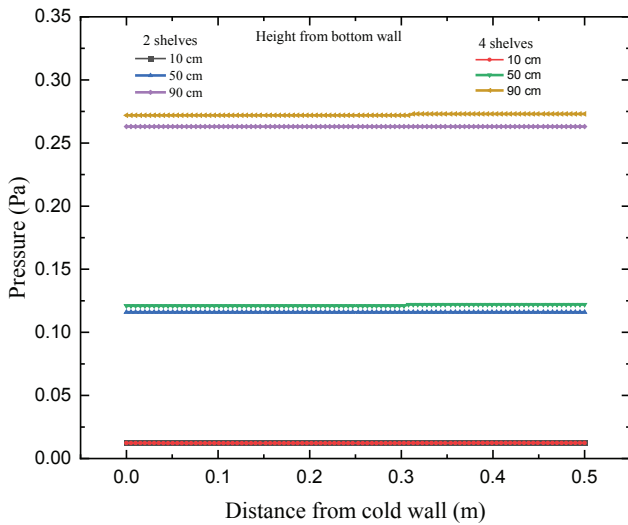


**Figure 15.** Pressure variations at different heights from the bottom wall in the refrigerating compartment with 2 shelves and 4 shelves.

Meanwhile, Figure 15 shows that the pressure in the middle of the refrigerating compartment with two shelves is less than in the middle of the refrigerating compartment with four shelves. For the refrigerating compartment with two and four shelves, the lowest pressure is obtained at the 10 cm height from the bottom wall. On the contrary, the maximum pressure is obtained as  $2.98 \times 10^{-1} Pa$  and  $3.07 \times 10^{-1} Pa$  for the compartment with two and four shelves, respectively, from the 90 cm height of the bottom wall.

Figure 16 shows the velocity vector of the refrigerating compartment with 2 and 4 shelves. The maximum air velocity of the refrigerating compartment with 2 plates is more

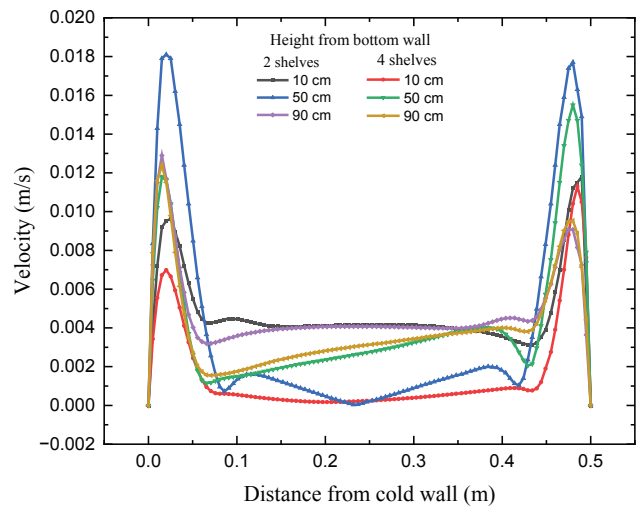


**Figure 17.** Air velocity at different heights from the bottom wall of the refrigerating compartment with 2 shelves and 4 shelves.

than that of the refrigerating compartment with 4 plates. Obstacles, like shelves, impact the airflow inside the compartment by reducing the airflow in the middle and affecting the air circulation in the boundary layers. The obstacles create additional gaps where air circulation occurs, leading to increased airflow in the refrigerating compartment.

Meanwhile, Figure 17 shows the air velocity at the different heights (0 cm, 5 cm, 10 cm, 30 cm, 50 cm, 70cm, 90 cm, 95 cm, and 100 cm) from the bottom wall of the refrigerating compartment without and with shelves, respectively. In the two figures, the air velocity near the cold wall and the hot wall is high. A little further away from the cold

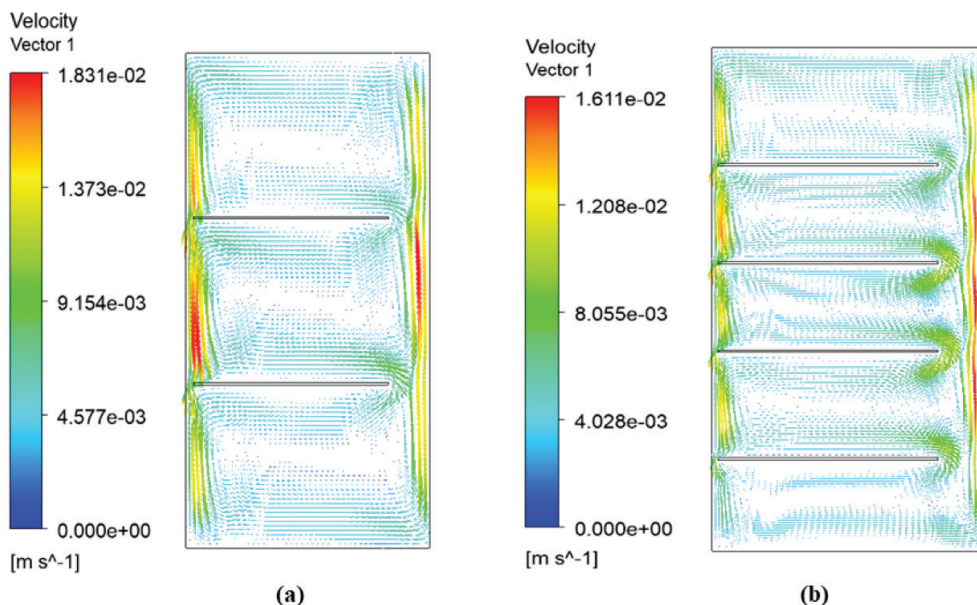


**Figure 16.** Velocity vector in refrigerating compartment; (a) 2 shelves and (b) 4 shelves.

wall, the air velocity decreases, and then the variation in velocity value is much less. Then the velocity increases as it approaches the hot wall. The velocity near the wall at the height of 50 cm from the bottom wall is maximum when two shelves in the refrigerating compartment with a maximum velocity of 0.018 m/s, while for four shelves compartment with the air velocity will be a maximum of 0.016 m/s.

## CONCLUSION

In this study, computational fluid dynamics simulations are employed to model airflow patterns, temperature gradients, and heat transfer mechanisms under various shelf configurations using ANSYS workbench 2020 R1. This study aimed to analyze temperature distribution and air flow for a model of household refrigerators, focusing on natural convection systems prevalent in refrigerators rather than forced convection systems. However, the momentous findings of this study are as follows:

- The analysis reveals significant temperature stratification: colder air tends to settle at the bottom, while warmer air accumulates at the top. Glass shelves are found to disrupt the primary airflow along the walls, but they also enhance heat transfer by improving airflow near the walls.
- The study evaluated the impact of glass shelves, both as enhancers of heat transfer due to improved wall airflow and as disruptors of central airflow patterns, thereby causing colder air stratification and influencing overall temperature uniformity.
- The lowest temperature is found at 272.55 K at 0 to 10 cm height from the bottom wall and the highest of 279.75 K at 95 to 100 cm height from the bottom wall due to the hot air rising upward and the cold air sinking downward, creating density variations in the compartment.
- The pressure range that was achieved in the refrigeration compartment without shelves and with four shelves is observed to be  $-7.11 \times 10^{-3}$  to  $2.88 \times 10^{-1}$  Pa and  $-7.95 \times 10^{-3}$  to  $3.07 \times 10^{-1}$  Pa, respectively. While the obtained maximum air velocity is found as  $1.87 \times 10^{-2}$  m/s and  $1.61 \times 10^{-2}$  m/s for without shelves and four shelves compartments, respectively.
- By focusing on a natural convection model without a fan, the research provided insights into optimizing refrigerator design to minimize warm regions and enhance natural convection heat exchange, thereby improving energy efficiency.

By applying the numerical approach, stakeholders in the refrigeration industry from designers to regulatory bodies can leverage detailed insights to drive advancements in appliance performance, energy efficiency, and food safety. The originality of this work lies in advancing beyond conventional forced convection models by exploring temperature stratification and natural convection effects to optimize shelf layout and improve energy efficiency. Future efforts could explore alternative shelving materials and configurations to further refine these findings and advance domestic refrigerator

technology toward more effective and sustainable cooling solutions. Investigate how different shelving materials with varying thermal conductivity and surface textures could offer insights into optimizing heat exchange efficiency and also explore optimal shelf configurations and placements within the refrigerator to minimize temperature differentials and enhance overall cooling efficiency. Moreover, evaluate the potential benefits of integrating active cooling technologies, such as fans or thermoelectric devices, to enhance natural convection and mitigate temperature stratification within the refrigerator compartment.

## NOMENCLATURE

$C_p$	Specific heat ( $J kg^{-1} K^{-1}$ )
$g$	Gravitational acceleration ( $m.s^{-2}$ )
$h$	Convective heat transfer coefficient ( $w m^{-2} K^{-1}$ )
$k$	Thermal conductivity ( $w m^{-1} K^{-1}$ )
$L$	Distance between the hot and cold wall ( $m$ )
$Nu$	Local Nusselt number
$Nu_{av}$	Average Nusselt number
$R_a$	Rayleigh number
$T$	Temperature ( $K$ )
$u$	Velocity along the x-axis ( $m.s^{-1}$ )
$v$	Velocity along the y-axis ( $m.s^{-1}$ )

### Greek symbols

$\alpha$	Thermal diffusivity ( $m^2.s^{-1}$ )
$\beta$	Coefficient of thermal expansion
$\vartheta$	Kinematic viscosity ( $m^2.s^{-1}$ )

### Subscripts

$H$	Hot wall
$C$	Cold wall

## AUTHORSHIP CONTRIBUTIONS

**Md. Ahsanul Bari (M. A. Bari):** Conceptualization, methodology, investigation, data acquisition, analysis, writing original draft, review, and editing manuscript.

**Dipayan Mondal (D. Mondal):** Conceptualization, methodology, investigation, analyzing and interpreting the data, writing, review and editing, discussion, supervising.

**Md. Abdul Hasib (M. A. Hasib):** Analyzing and interpreting the data, reviewing and editing, and writing.

## DATA AVAILABILITY STATEMENT

Data will be available upon reasonable request from the corresponding author.

## CONFLICT OF INTEREST

The authors declared no conflicts of interest associated with this publication, and there had been no significant financial support for this work that could have influenced its outcome.

## ETHICS

There are no ethical issues with the publication of this manuscript.

## REFERENCES

- [1] IIF-IIR. Report on refrigeration sector achievements and challenges. *World Summit Sustain Dev* 2002;33:1-78.
- [2] Laguerre O, Ben Amara S, Moureh J, Flick D. Numerical simulation of air flow and heat transfer in domestic refrigerators. *J Food Engineer* 2007;81:144-156. [\[CrossRef\]](#)
- [3] Laguerre O, Flick D. Heat transfer by natural convection in domestic refrigerators. *J Food Engineer* 2004;62:79-88. [\[CrossRef\]](#)
- [4] Billiard F. Refrigerating equipment, energy efficiency and refrigerants. *Bull Int Inst Refrig* 2005;85:1-7.
- [5] Laguerre O, Ben Amara S, Flick D. Experimental study of heat transfer by natural convection in a closed cavity: application in a domestic refrigerator. *J Food Engineer* 2005;70:523-537. [\[CrossRef\]](#)
- [6] Karayiannis TG, Ciofalo M, Barbaro G. On natural convection in a single and two zone rectangular enclosure. *Int J Heat Mass Transf* 1992;35:1645-1657. [\[CrossRef\]](#)
- [7] Betts PL, Bokhari IH. Experiments on turbulent natural convection in an enclosed tall cavity. *Int J Heat Fluid Flow* 2000;21:675-683. [\[CrossRef\]](#)
- [8] Bansal PK, Wich T, Browne MW. Optimisation of egg-crate type evaporators in domestic refrigerators. *Appl Therm Engineer* 2001;21:751-770. [\[CrossRef\]](#)
- [9] Masjuki HH, Saidur R, Choudhury IA, Mahlia TMI, Ghani AK, Maleque MA. The applicability of ISO household refrigerator-freezer energy test specifications in Malaysia. *Energy* 2001;26:723-737. [\[CrossRef\]](#)
- [10] Ding GL, Qiao HT, Lu ZL. Ways to improve thermal uniformity inside a refrigerator. *Appl Therm Engineer* 2004;24:1827-1840. [\[CrossRef\]](#)
- [11] Hermes CJL, Melo C, Knabben FT, Gonçalves JM. Prediction of the energy consumption of household refrigerators and freezers via steady-state simulation. *Appl Energy* 2009;86:1311-1319. [\[CrossRef\]](#)
- [12] Yang KS, Chang WR, Chen IY, Wang CC. An investigation of a top-mounted domestic refrigerator. *Energy Conver Manage* 2010;51:1422-1427. [\[CrossRef\]](#)
- [13] Bayer O, Oskay R, Paksoy A, Aradag S. CFD simulations and reduced order modeling of a refrigerator compartment including radiation effects. *Energy Conver Manage* 2013;69:68-76. [\[CrossRef\]](#)
- [14] Yan G, Chen Q, Sun Z. Numerical and experimental study on heat transfer characteristic and thermal load of the freezer gasket in frost-free refrigerators. *Int J Refrig* 2016;63:25-36. [\[CrossRef\]](#)
- [15] Avci H, Kumlutaş D, Özer Ö, Özşen M. Optimisation of the design parameters of a domestic refrigerator using CFD and artificial neural networks. *Int J Refrig* 2016;67:227-238. [\[CrossRef\]](#)
- [16] Gao F, Shoai Naini S, Wagner J, Miller R. An experimental and numerical study of refrigerator heat leakage at the gasket region. *Int J Refrig* 2017;73:99-110. [\[CrossRef\]](#)
- [17] Mansouri R, Bourouis M, Bellagi A. Experimental investigations and modelling of a small capacity diffusion-absorption refrigerator in dynamic mode. *Appl Therm Engineer* 2017;113:653-662. [\[CrossRef\]](#)
- [18] Ledesma S, Belman-Flores JM. Mathematical application to analyze the thermal behavior of a domestic refrigerator: influence of the location of the shelves. *Int J Refrig* 2017;74:362-370. [\[CrossRef\]](#)
- [19] Söylemez E, Alpman E, Onat A, Yükselentürk Y, Hartomacıoğlu S. Numerical (CFD) and experimental analysis of hybrid household refrigerator including thermoelectric and vapour compression cooling systems. *Int J Refrig* 2019;99:300-315. [\[CrossRef\]](#)
- [20] Gulmez M, Yilmaz D. Design and development of a refrigerator door gasket to prevent condensation. *Heat Transf Res* 2020;51:1061-1072. [\[CrossRef\]](#)
- [21] Li Z, Ding G, Miao S, Han X. Development of novel air distributor for precise control of cooling capacity delivery in multi-compartment indirect cooling household refrigerators. *Int J Refrig* 2020;119:175-183. [\[CrossRef\]](#)
- [22] Wie JH, Cho HW, Park YG, Kim YS, Seo YM, Ha MY. Temperature uniformity analysis of a domestic refrigerator with different multi-duct shapes. *Appl Therm Engineer* 2021;188:116604. [\[CrossRef\]](#)
- [23] Logeshwaran S, Chandrasekaran P. CFD analysis of natural convection heat transfer in a static domestic refrigerator. *IOP Conf Ser Mater Sci Engineer* 2021;1130:012014. [\[CrossRef\]](#)
- [24] Cui P, He L, Mo X. Flow and heat transfer analysis of a domestic refrigerator with complex wall conditions. *Appl Therm Engineer* 2022;209:118306. [\[CrossRef\]](#)
- [25] Jalili B, Jalili P. Numerical analysis of airflow turbulence intensity effect on liquid jet trajectory and breakup in two-phase cross flow. *Alexandria Engineer J* 2023;68:577-585. [\[CrossRef\]](#)
- [26] Jalili P, Ganji DD, Nourazar SS. Investigation of convective-conductive heat transfer in geothermal system. *Results Phys* 2018;10:568-587. [\[CrossRef\]](#)
- [27] Jalili P, Kazerani K, Jalili B, Ganji DD. Investigation of thermal analysis and pressure drop in non-continuous helical baffle with different helix angles and hybrid nano-particles. *Case Stud Therm Engineer* 2022;36:102209. [\[CrossRef\]](#)
- [28] Jalili B, Aghaee N, Jalili P, Domiri Ganji D. Novel usage of the curved rectangular fin on the heat transfer of a double-pipe heat exchanger with a nanofluid. *Case Stud Therm Engineer* 2022;35:102086. [\[CrossRef\]](#)

- [29] Salehipour D, Jalili B, Jalili P. Effect of humidification of combustion products in the boiler economizer with spiral geometry. *Results Engineer* 2024;21:101906. [\[CrossRef\]](#)
- [30] Sun SL, Liu D, Wang YZ, Kim HB, Hassan M, Hong HJ. Heat transfer performance prediction of Taylor-Couette flow with longitudinal slits using artificial neural networks. *Appl Therm Engineer* 2023;221:119792. [\[CrossRef\]](#)
- [31] Mondal D, Alam A, Islam MA. Experimental observation of a small capacity vapor absorption cooling system. *Int J Sci Engineer Res* 2024;5:456-467.
- [32] Mondal D, Ikram MO, Rabbi MF, Moral MNA. Experimental investigation and comparison of bend tube parallel & counter flow and cross flow water to air heat exchanger. *Int J Sci Engineer Res* 2014;5:686-695.
- [33] Mondal D, Islam MA. Experimental investigation on an intermittent ammonia absorption refrigeration. *Mech Engineer Res J* 2018;11:59-65.
- [34] Mondal D, Hori Y, Kariya K, Miyara A, Jahangir Alam M. Measurement of viscosity of a binary mixture of R1123 + R32 refrigerant by tandem capillary tube method. *Int J Thermophys* 2020;41:1-20. [\[CrossRef\]](#)
- [35] Mondal D, Kariya K, Tuhin AR, Amakusa N, Miyara A. Viscosity measurement for trans-1,1,1,4,4,4-hexafluoro-2-butene(R1336mzz(E)) in liquid and vapor phases. *Int J Refrig* 2022;133:267-275. [\[CrossRef\]](#)
- [36] Mondal D, Kariya K, Tuhin AR, Miyoshi K, Miyara A. Thermal conductivity measurement and correlation at saturation condition of HFO refrigerant trans-1,1,1,4,4,4-hexafluoro-2-butene (R1336mzz(E)). *Int J Refrig* 2021;129:109-117. [\[CrossRef\]](#)
- [37] Mondal D, Tuhin AR, Kariya K, Miyara A. Measurement of kinematic viscosity and thermal conductivity of 3,3,4,4,5,5-HFCPE in liquid and vapor phases. *Int J Refrig* 2022;140:150-165. [\[CrossRef\]](#)
- [38] Das P, Mondal D, Islam A, Afroj M. Thermodynamic performance evaluation of a solar powered Organic Rankine cycle (ORC) and dual cascading vapor compression cycle (DCVCC): Power generation and cooling effect. *Energy Conver Manage* 2024;23:100662. [\[CrossRef\]](#)
- [39] Yilmaz H, Erbay LB, Dogan B. Numerical investigation of the bottom cabinet of a household refrigerator. *J Therm Engineer* 2016;2:946-953. [\[CrossRef\]](#)
- [40] Roy PC, Kundu B. Thermodynamic modeling of a pulse tube refrigeration system. *J Therm Engineer* 2018;4:1668-1679. [\[CrossRef\]](#)
- [41] Choudhari M, Gawali B, Malwe P, Deshmukh N, Dhalait R. Second order cyclic analysis of counter flow pulse tube refrigerator. *J Therm Engineer* 2023;9:580-592. [\[CrossRef\]](#)
- [42] Özkan DB, Ünal F. Energy consumption of defrosting process in no-frost refrigerators. *J Therm Engineer* 2018;4:2445-2450. [\[CrossRef\]](#)
- [43] Shikalgar ND, Sapali SN. Energy and exergy analysis of a domestic refrigerator: Approaching a sustainable refrigerator. *J Therm Engineer* 2019;5:469-481. [\[CrossRef\]](#)
- [44] Kumar V, Karimi MN, Kamboj SK. Comparative analysis of cascade refrigeration system based on energy and exergy using different refrigerant pairs. *J Therm Engineer* 2020;6:106-116. [\[CrossRef\]](#)
- [45] Arslan E, Kosan M, Aktas M, Erten S. Experimental assessment of comparative R290Vs. R449a refrigerants by using 3E (energy, exergy and environment) analysis: A supermarket application. *J Therm Engineer* 2021;7:595-607. [\[CrossRef\]](#)
- [46] Gugulothu SK. Enhancement of household refrigerator energy efficiency by studying the effect of refrigerant charge and capillary tube length. *J Therm Engineer* 2021;7:1121-1129. [\[CrossRef\]](#)
- [47] Illyas SM, Vellaisamy K, Muthumanokar A. Numerical analysis on heat transfer, flow structure and exergy loss of combined truncated and circular ribs in a square duct. *J Therm Engineer* 2023;9:1585-1603. [\[CrossRef\]](#)
- [48] Shariar T, Mondal D, Hasib A, Islam A. Effects of gas-liquid flow and dehumidification performance of a liquid desiccant dehumidifier: A numerical approach for vertical smooth & rough, and inclined rough plates. *J Therm Engineer* 2024. Doi: 10.14744/thermal.0000883. [Epub Ahead of Print.]
- [49] Hmood KS, Apostol V, Pop H, Badescu V, Pop E. Drop-in and retrofit refrigerants as replacement possibilities of R134a in domestic/commercial refrigeration and automobile air conditioner applications. *J Therm Engineer* 2021;7:1815-1835. [\[CrossRef\]](#)
- [50] Gambhir D, Sherwani AF, Arora A, Ashwni. Parametric optimization of blowdown operated double-effect vapour absorption refrigeration system. *J Therm Engineer* 2022;8:78-89. [\[CrossRef\]](#)
- [51] Deshmukh MS, Deshmukh DS, Chavhan SP. A critical assessment of the implementation of phase change materials in the VCC of refrigerator. *J Therm Engineer* 2022;8:562-572. [\[CrossRef\]](#)
- [52] Hasheer SKM, Kolla S, Rao DK, Ram YN. Theoretical exploration of low GWP refrigerant mixtures as replacement to HFC-134A in a vapour compression refrigeration system. *J Therm Engineer* 2023;9:912-920. [\[CrossRef\]](#)
- [53] Ugudur B, Direk M. Comparative evaluation of experimental ejector refrigeration system for different operating configurations. *J Therm Engineer* 2023;10:321-329. [\[CrossRef\]](#)
- [54] Shahini N, Karami M, Behabadi MAA. Numerical investigation of direct absorption evacuated tube solar collector using alumina nanofluid. *J Therm Engineer* 2024;10:562-571. [\[CrossRef\]](#)
- [55] Islam L, Mondal D, Islam A, Das P. Effects of heat transfer characteristics of R32 and R1234yf with Al<sub>2</sub>O<sub>3</sub> nanoparticle through U-bend tube evaporator. *J Engineer* 2024:9991809. [\[CrossRef\]](#)



- 
- [56] Srivastava A, Maheshwari M. Energy, exergy and economic analysis of ammonia-water power cycle coupled with trans-critical carbon di-oxide cycle. *J Therm Engineer* 2024;10:599-612. [\[CrossRef\]](#)
- [57] Srivastava A, Maheshwari M. Thermodynamic analysis of solar assisted binary vapour cycle using ammonia-water mixture and transcritical CO<sub>2</sub>: A review. *J Therm Engineer* 2024;10:790-810. [\[CrossRef\]](#)
- [58] Amin MT. Performance analysis of a new combined absorption-adsorption refrigeration system to improve energy performance. *J Therm Engineer* 2024;10:722-736. [\[CrossRef\]](#)
- [59] Inam MI. Direct numerical simulation of laminar natural convection in a square cavity at different inclination angle. *J Engineer Adv* 2020;01:23-27. [\[CrossRef\]](#)
- [60] Davis GdV. Laminar natural convection in an enclosed rectangular cavity. *Int J Heat Mass Transf* 1968;11:1675-1693. [\[CrossRef\]](#)
- [61] Rincón-Casado A, Sánchez de la Flor FJ, Chacón Vera E, Sánchez Ramos J. New natural convection heat transfer correlations in enclosures for building performance simulation. *Engineer Appl Comp Fluid Mech* 2017;11:340-356. [\[CrossRef\]](#)